46th AIAA/ASME/SAE/ASEE Joint Propulsion Conference & Exhibit
25 - 28 July 2010, Nashville, TN

AIAA 2010-6530

Evaluation of discharge behavior of the pulsed plasma thruster SIMP-LEX

Tony Schönherr* and Kimiya Komurasaki†
The University of Tokyo, Kashiwa, Chiba, 277-8561, Japan

Rei Kawashima‡ and Yoshihiro Arakawa§
The University of Tokyo, Bunkyo, Tokyo, 113-8656, Japan

Georg Herdrich¶
Universität Stuttgart, Stuttgart, Baden-Württemberg, 70569, Germany

The pulsed plasma thruster ADD SIMP-LEX, developed at the IRS, was investigated at the University of Tokyo to further characterize the thruster's performance and discharge behavior. This was done by experimental investigation of configurations with a different amount of capacitors and discrete applied voltages. To do so, a measurement system for the discharge current and the optical properties was built up and successfully applied. Further, the numerical model for the prediction of the current-normalized magnetic flux density was improved and the convergence properties of the integration towards the change in inductance studied. From the discharge current waveforms and the pictures taken from the propagating plasma, information about the amount of plasma creations, their propagation velocity and the oscillation behavior was deducted. For further characterization, the energy transfer efficiency and the electrical efficiency was derived from these data, leading to a tool to compare different configurations. It was found, that a middle voltage yields higher electrical efficiencies of about 40% whereas the energy transfer efficiency is higher the lower the applied voltage.

Nomenclature

α	Half divergence angle
δ	Grid size
η_{acc}	Acceleration efficiency
η_{div}	Beam divergence efficiency
η_{el}	Electrical efficiency
η_{tran}	Energy transfer efficiency
η_t	Thrust efficiency
Ψ	Current action integral
B	Magnetic flux density
I	Discharge current
I_{peak}	Peak value of discharge current
ΔL	Change in inductance
l_{char}	Characteristic length
m_{bit}	Ablated mass shot

*Ph.D. student, Department of Advanced Energy, Kashiwa-no-ha 5-1-5, Kiban-tou 313, 277-8561 Kashiwa, Japan, schoenherr@al.t.u-tokyo.ac.jp, and Student Member AIAA.
†Professor, Department of Advanced Energy, Senior Member AIAA.
‡Graduate Student, Department of Aeronautics and Astronautics, Hongo 7-3-1, 113-8656 Bunkyo, Japan
§Professor, Department of Aeronautics and Astronautics, and Senior Member AIAA.
¶Associate Professor, Head Plasma Wind Tunnels and Electric Propulsion, Institute for Space Systems (IRS), Pfaffenwaldring 31, 70569 Stuttgart, Germany, Senior Member AIAA

t Discharge time

I. Introduction

The Institute of Space Systems (IRS) of the Universität Stuttgart in Germany is undergoing the challenge of realizing several small satellites within the Stuttgart Small Satellite Program.[1] The LEO satellite *Perseus* is planned to comprise one thermal arcjet thruster named Talos and one pulsed MPD thruster named Simp-lex, both developed and studied at IRS in close national and international collaboration.[2,3] An important mission objective is the intense evaluation of the on-board electric propulsion systems in regard to operativeness, compatibility and reliability for space application. Pulsed magnetoplasmadynamic thrusters, usually referred to as PPT (Pulsed Plasma Thruster), are promising candidates for usage on board small satellites due to the robust and simple design and the very low requirements in the power consumption. They consist of a capacitor bank, a pair of electrodes, an ignition device and the propellant, and create most of their thrust by acceleration of charged species by Lorentz force in a short-time discharge.
PPT can be classified depending on their design (parallel plate, coaxial), on the propellant (ablative, liquid propellant, gas-fed), on the propellant feed (breech-fed, side-fed), on the ignition method (spark plug, laser) or on the main acceleration method (electromagnetic, electrothermal). Further, size and energy level have significant influence on performance and quality of the thruster.
Due to imperfect acceleration and phenomena like late-time ablation, pulsed MPD thrusters often suffer from low thrust efficiency. Optimization was conducted at IRS with geometric and electric aspects to improve this thrust efficiency, eventually leading to a new engineering model named Add Simp-lex[4,5] showing a tremendously higher efficiency. Investigations showed that not only the energy itself but also the balance between capacitance and voltage have an influence on the final performance of the thruster, i.e., impulse bit and ablated mass shot. While a higher energy in a general sense does lead to a higher efficiency, additional gain can be achieved by distributing this energy thoughtfully. To entirely understand the phenomena happening during the discharge and the influence of energy-related parameters on the thruster behavior, additional measurements of discharge current and plasma propagation speed were seen necessary and conducted within a mutual collaboration at the University of Tokyo.[6] A Rogowski coil and a high-speed camera with wavelength filters were used for these purposes, and were applied to thruster configurations with varying voltage and amount of capacitors. The magnetic flux density and the derived change in inductance during the plasma acceleration were calculated using the Biot-Savart law and a numerical integration, with the aim of providing input data for the performance model[7] and to enable calculation of the electrical efficiency. Further investigations of the plasma creation and spread were conducted to insightfully characterize the thruster. Information about the energy transfer efficiency, the electrical efficiency and the propagations speeds for different thruster setups were derived and compared. The goal of this study is to understand not only how but also why the energy distribution affects the performance for a small energy thruster.

II. Experimental setup

Experiments were conducted at the Department of Advanced Energy of the University of Tokyo. The vacuum chamber used is evacuated by means of a rotary vane pump and a turbomolecular pump providing a throughput of 2.2 $\times 10^{-3}$ Pa m^3/s at 0.01 Pa. Typical background pressure during experiment was 5 $\times$ 10^{-2} Pa. The thruster model used for the experiments is an identical setup of Add Simp-lex as used at IRS in Stuttgart.[6,8] It is shown in Figure 1.
The engineering model consists of up to 4 capacitors à 20 µF and can be charged up to 1300 V. Anode and cathode are connected to the capacitors' pins with shortest current paths, are made of copper and insulated by Kapton™ foil. The pure Teflon™ propellant is placed in between the electrodes in a side-fed configuration. For the experiments conducted, the voltage was varied between 500 and 1300 V for configurations of 1 and 4 capacitors. No propellant feed system was needed as only few pulses were conducted for the calibration of the current probe, and the evaluation of the different thruster configurations. Voltage measurement was conducted by a Yokogawa 700924 differential high voltage probe.

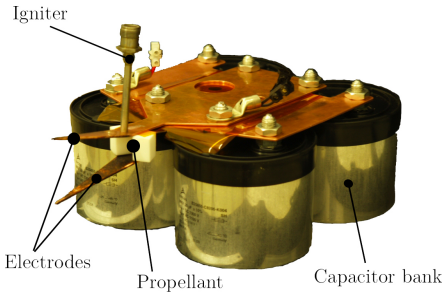

Figure 1. Setup of Add Simp-lex.

II.A. Current measurement

Due to the limiting geometry of ADD SIMP-LEX, the discharge current was measured by an in-house Rogowski coil,[9] placed in a shielding box and around the pin of one of the capacitors as can be seen in Figure 2. The anode electrode is then placed directly upon the box separated by KAPTON foil.
The output signal was then lead by BNC cables to avoid strong electromagnetic noise. A passive RC circuit was used for integration of the signal. Calibration was conducted and a sensitivity of about 10,000 A/V derived.

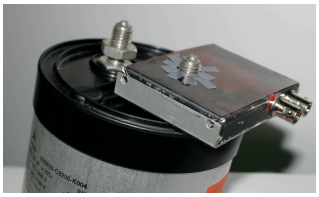

Figure 2. Position of Rogowski coil.

II.B. Optical measurement

A high-speed camera of type *Ultra-8* was used to record pictures of the plasma propagation. A Nikon 85mm f/1.8 lens was used to focus the image of the center plane of the electrodes. Two different filters were put into the optical path to enable observation of a distinct plasma species. At a wavelength of 426.8 nm, simple ionized carbon (C^+) emits very intensively, so a filter for this species was used to identify the charged particle front whereas a filter for 514.5 nm was used to determine the strong emission line of excited diatomic carbon (C_2), as representative of the neutral particles.
Eight pictures with a resolution of 520 × 520 pixel were taken at an exposure time of 100 ns and a frame speed of 5 Mfps. Brightness of the pictures was adjusted by regulating the aperture of the lens, and the gain of the camera sensor respectively. While using the filters, the brightness of the picture decreased a lot yielding the need for an aperture of f/1.8 and using a high gain. This eventually results in slightly blurry and noisy images.

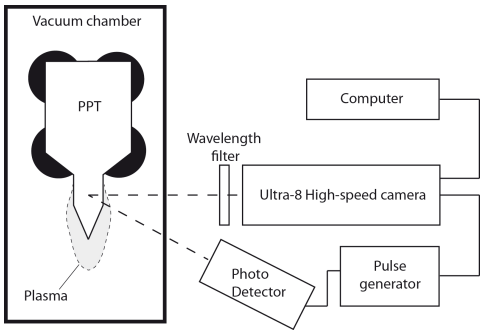

Figure 3. Optical setup.

Triggering of the camera was done by a pulse generator which itself was triggered by a photo detector pointed towards the center of the discharge space. That means that there is a minimum hardware delay making it impossible to see the very first few 100 ns of the discharge. However, due to the side-fed thruster configuration the plasma is blocked from view by the propellant bar thus, no information about the plasma propagation was lost.
The optical setup is summarized in Figure 3.

III. Model for magnetic field

To calculate the magnetic flux density and the resulting change in inductance during the discharge of a pulsed plasma thruster, and particularly for SIMP-LEX, a calculation method was derived in previous work[4,7,10] using either Ampère's law applied to infinite current filaments or the Biot-Savart law. It was modified to handle the flared and pointed electrode geometry eventually leading to an increase in computation time which lead to a reduction of the grid finesse. However, it was found that convergence of the results for some geometries could not be guaranteed.
Modifications and optimization of the computational code were conducted with the aim of reducing the time needed. Especially, an improvement of variable and memory management, algorithm operations and the integration method used to calculate the magnetic flux density based on geometry yielded significant savings in computational load. A transition to Fortran 90, being more suited to this amount of mathematical operations, and the extension of the computation on a cluster improved the calculation time furthermore. That is, it was possible to compute finer grids and verify whether or not the calculation is converging.
As was shown previously,[4] the magnetic flux density can be integrated towards the change in inductance which is a result of the propagating plasma, the current sheet respectively. This integration could be done partially analytically for the calculation method using Ampère's law, but is entirely numerical in case of the Biot-Savart law. The first step to investigate the convergence of the computation was to verify whether the integration method itself is converging. For this reason, the following four methods have been applied and compared: composed Simpson's rule (S), composed Simpson's 3/8 rule (S3/8), Newton-Cotes formulas (NC) and the Clenshaw-Curtis integration (CC).[11] Figure 4 shows the results of the computations for different grid

sizes and the geometry of Add Simp-lex. The change in inductance computed for the case when the current sheet reaches the tip of the electrodes is plotted against the grid size, i.e., the reciprocal of the number of grid points. For the first 3 integration methods no convergence could be deducted whereas the Clenshaw-Curtis algorithm shows very good converging properties. It was, hence, selected for further calculations.

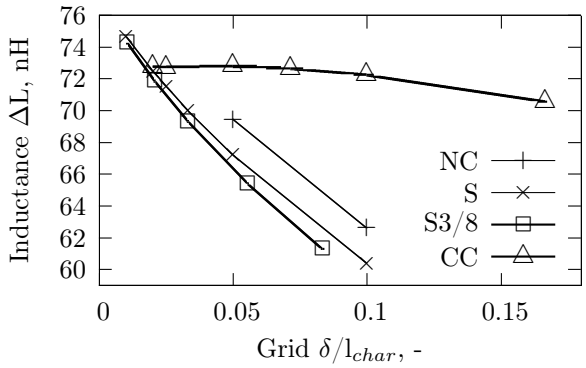

Figure 4. Change in inductance for different integration methods and varying grid sizes

Adding a current sheet to the calculation process introduced some strong gradients in the magnetic flux density yielding small instabilities in the numerical integration. Therefore, convergence was investigated for different current sheet thicknesses and types (adaptive or static). An example on how the magnetic flux density is distributed in between the electrodes is shown in Figure 5 for the case with and without current sheet.

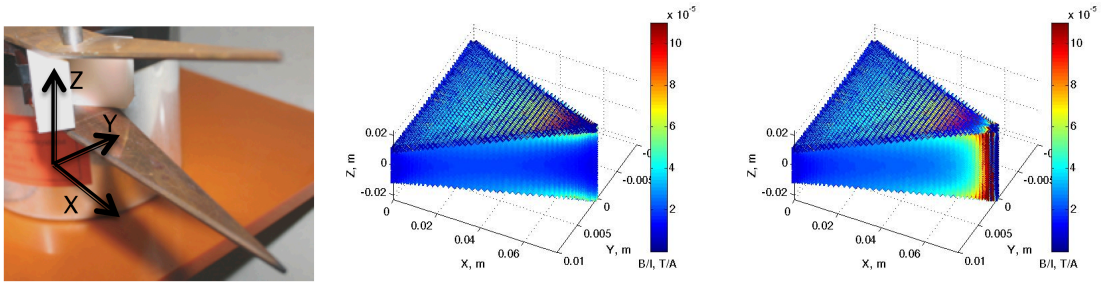

(a) Inter-electrode space in detail (b) Magnetic flux density neglecting current sheet (c) Magnetic flux density respecting current sheet

Figure 5. Calculated normalized magnetic flux densities for Add Simp-lex.

From Figure 6(a), it can be deducted that a finer grid is required for any of the cases of sheet thickness than compared to the case without a current sheet. In the case of the geometry of Add Simp-lex, an increase in grid points beyond 50 for each coordinate axis yielded but a slight change in the results as can be seen in Figure 6(b). That means that further calculations can be done with a grid of 50^3 grid points to guarantee a converged result.
With these efforts, not only the accelerating fraction of the magnetic flux density can be calculated, but also the change in inductance, crucial for further calculations, can be estimated more precisely.

IV. Results and Discussion

IV.A. Current measurement

Measuring the discharge current and voltage alike gives information about the oscillation behavior and the peak currents occurring during the breakdown. These information are evident, as they enable a judgement whether a PPT is well optimized and efficiently working. Although the maximum value is already interesting, in order to compare the discharge behavior of different configurations, it is better to normalize the plots by their peak value. Thruster configurations with one and four capacitors were investigated for applied voltages between 500 and 1300 V. Figures 7(a) and 7(b) show the normalized results. For the sake of better visibility,

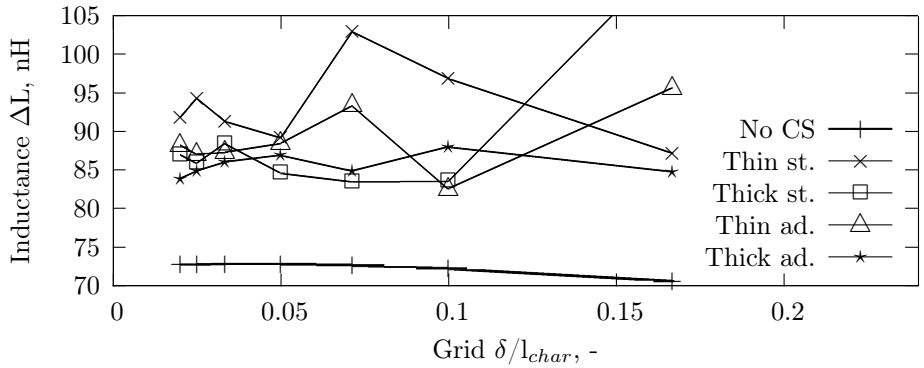

(a) Change in inductance for cases with included current sheet

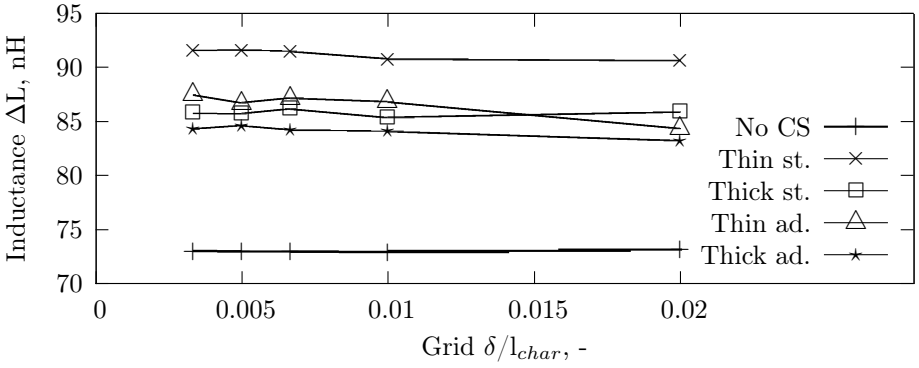

(b) Finer grid results

Figure 6. Convergence study results for different current sheet thicknesses. "No CS" = No current sheet, "st." = static, and "ad." = adaptive

only selected voltages are shown.

It is obvious that an increase in discharge voltage yields a less-damped oscillation. This is linked to a second or even third plasma creation and acceleration. As energy increases, the current density in the discharge space varies, and further plasma can be created. Introducing more capacitors increases not only the capacitance, but also changes the circuit resistance and inductance of the thruster. Hence, a more-damped oscillation can be observed in this configuration. Due to the higher damping, the peak value of the

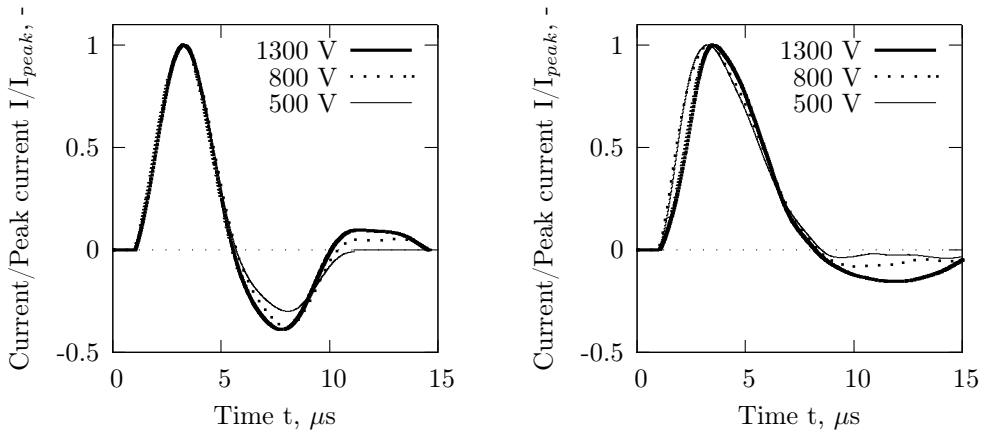

(a) Normalized discharge currents for 1 capacitor

(b) Normalized discharge currents for 4 capacitors

Figure 7. Normalized discharge current waveforms

discharge current increases only by a factor of 2.5 than compared to the 4-times higher energy stored in the capacitor bank, leading to a maximum value of 25 kA at the 68 J configuration. As the Lorentz force is proportional to the current density, one would then expect a higher oscillation to be favorable. However, previous thruster investigations[5,12] have shown that performance, i.e. impulse bit and thrust efficiency, is improved for a higher damping coefficient. Furthermore, additional oscillations badly affect the capacitors and increase energy losses.[13] A value to characterize the thruster configuration is the so-called current action integral Ψ, defined as:[14,15]

$$\Psi = \int_0^\infty I^2 \, \mathrm{d}t. \tag{1}$$

Information about this value, and the influence of parameters on it, can yield conclusions about the impulse bit, and the mass bit respectively.[16–18] However, the equations presented by Palumbo and Guman, neglect edge effects of the electrodes on the magnetic flux density which is a too strong simplification of the calculation method explained in Section III. Nevertheless, general tendencies can be derived. The values were computed for different thruster setups and normalized by the amount of capacitors used, and are shown in Figure 8.

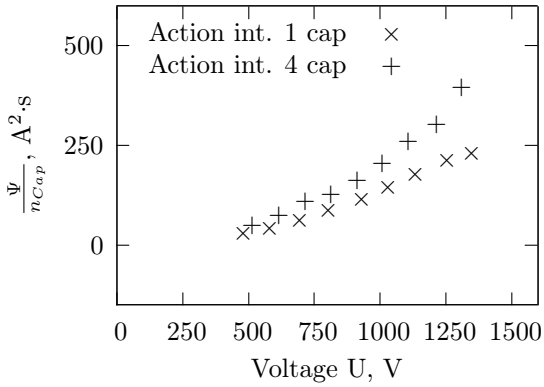

Figure 8. Current action integrals for different voltages and capacitors

From this data, it can be seen that the current action integral per capacitor is higher for the higher-damped oscillation of the configuration with 4 capacitors. That is, a higher impulse bit and mass bit per capacitor could be expected which would influence the thrust efficiency eventually. According to Palumbo and Guman,[16] the ablated mass shot would be proportional to the current action integral and the ratio of the propellant surfaces. The latter were not changing during the experiments herein. Dividing the mass shot and the impulse bit[5] by the measured current action integral yields the values shown in Table 1.

Table 1. Mass shots, impulse bits and calculated proportionality factors for U=1300 V

	1 capacitor	4 capacitors
m_{bit}, µg	17.3	53.4
I_{bit}, µNs	342	1370
Ψ, $A^2 \cdot$ s	230	1580
m_{bit}/Ψ, ng/($A^2 \cdot$ s)	75	34
I_{bit}/Ψ, µN/(A^2)	1.5	0.9

The proportionality factor for the mass shot is more than twice as high for the thruster with only one capacitor whereas the impulse bit changes by a factor of roughly 1.5. That means that the proportionality factor is strongly dependent on the properties of the thruster, and of the oscillation circuit respectively. It is further possible to conclude that the acceleration is indeed higher for the weakly damped case, but that also much more mass is ablated and probably not accelerated and by that negatively influencing the overall performance. Introducing more capacitors is not only affecting the capacitance of the system, but also introduces inductance and resistance influencing the damping coefficient but also the plasma creation. As the plasma itself introduces resistance and inductance, the possible effect on the overall behavior is difficult

to predict without a proper understanding of the ablation process and the electrical properties of the circuit and the plasma. For this sake, Palumbo and Guman[14] showed a method to derive the initial inductance of the system leading to values of 214±7 nH for the one-capacitor case, and 93±8 nH for the four-capacitor case respectively. This lower inductance increases the damping coefficient of the oscillation circuit.

IV.B. High-speed camera

With help of the high-speed camera system explained in Section II.B, pictures of the plasma creation and propagation could be recorded for different voltages and capacitances, and with and without application of wavelength filters. As an example, the post-processed pictures for the 3 filter cases (without, C^+, C_2) of the [4 cap - 1300 V]-configuration are shown in Figures 9 and 10. Therein, the plasma is propagating to the left, showing the cathode in the upper half, and the anode in the lower half. The post-processing was done in a way, so that the brightest part of the picture is associated to "red" whereas the dark parts are represented by "blue".
During the first few µs of the discharge, a very bright plasma phenomenon can be observed close to the cathode. This is strongly visible while using the filter for C^+, implying the presence of charged particles accelerated by the magnetic field, and attracted to the cathode by the still-present electric field. Hence, the so-called current sheet canting occurs. However, a distinct current sheet cannot be observed for the first plasma phenomenon. After the first 5 µs, almost no light is emitted anymore at the wavelength of C^+. As the discharge current has already past its maximum at that time (refer to Figure 7(b)), the following current density is not sufficient to yield ionized particles. Nevertheless, neutral particles are ablated and propagated by thermal expansion, and light is then emitted by the excited matter even after the discharge current ceases. A distinct current sheet of about 2 mm thickness could be observed for this part of the plasma, as acceleration forces do not distort the sheet to a diffuse one. Comparing with the discharge current, this means that the negative part of the current waveform does not significantly contribute to the thrust creation as almost no charged particles are created and accelerated, but only a neutral plasma fraction. For the other thruster configurations, similar observations were done. In case of the [1 cap - 1300 V]-configuration, however, a second, slower plasma phenomenon was observed, complying with the more oscillating character of the discharge current (Figure 7(a)).

From the pictures taken, the propagation velocity of the plasma in the thrust direction was derived for the different thruster setups. However, due to the changes in brightness between the frames, plasma canting effects, inhomogeneous lighting and a diffuse current sheet, the measurement was strongly defied. Table 2 shows the estimated plasma velocities for the main plasma propagation, as well as for the second plasma creation for the [1 cap - 1300 V]-configuration, and the thermally accelerated neutral particles for the [4 cap - 1300 V]-configuration.

Table 2. Plasma propagation velocities, in km/s

	1 capacitor	4 capacitors
500 V	24.6	43.1
900 V	40.7	55.4
1300 V	35.6 (first)	25.7 (plasma)
	25.9 (second)	1.3 (thermal)

The values show that the highest velocities are found in the middle voltage range whereas for higher energies, more mass is ablated and, thus, not accelerated equivalently. Further, it can be derived that the second plasma phenomenon is not accelerated as much as the first one, as the lower peak current does indicate.

Taking a picture from an lower view of the thruster yields information about the divergence of the plasma beam. For a configuration with U=1300 V and 4 capacitors, Figure 11 shows the raw image and a strongly post-processed picture of the first plasma phenomenon. An angle of 2α= 11.5 deg was measured, resulting in a beam divergence efficiency of:

$$\eta_{div} = \left(\frac{1}{2}(1+\cos^2\alpha)\right)^2 = 96\%. \tag{2}$$

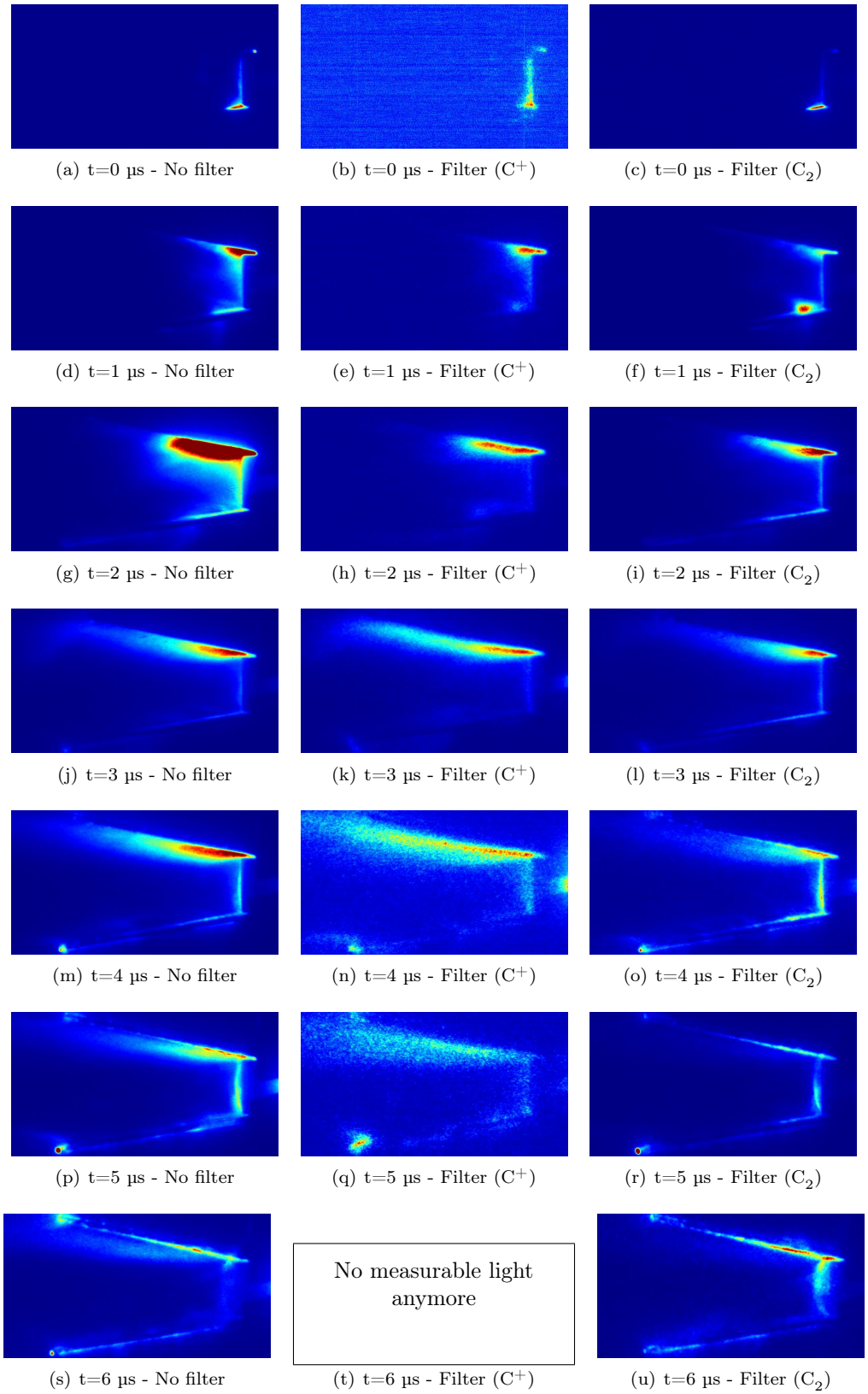

(a) t=0 µs - No filter (b) t=0 µs - Filter (C^+) (c) t=0 µs - Filter (C_2)

(d) t=1 µs - No filter (e) t=1 µs - Filter (C^+) (f) t=1 µs - Filter (C_2)

(g) t=2 µs - No filter (h) t=2 µs - Filter (C^+) (i) t=2 µs - Filter (C_2)

(j) t=3 µs - No filter (k) t=3 µs - Filter (C^+) (l) t=3 µs - Filter (C_2)

(m) t=4 µs - No filter (n) t=4 µs - Filter (C^+) (o) t=4 µs - Filter (C_2)

(p) t=5 µs - No filter (q) t=5 µs - Filter (C^+) (r) t=5 µs - Filter (C_2)

(s) t=6 µs - No filter (t) t=6 µs - Filter (C^+) (u) t=6 µs - Filter (C_2)

Figure 9. Pictures taken with high-speed camera and 2 different filters for U=1300 V, 4 capacitors.

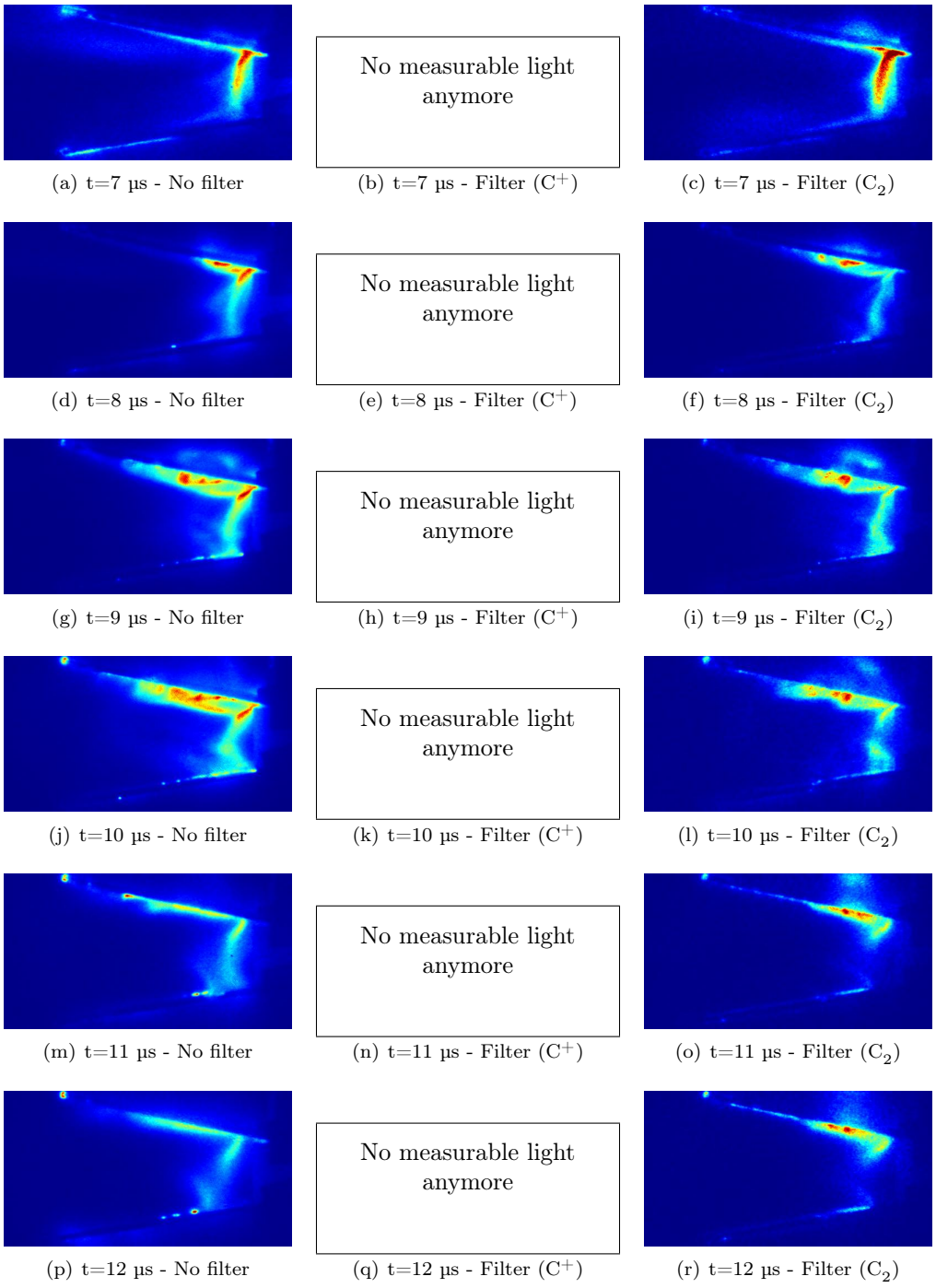

(a) t=7 µs - No filter (b) t=7 µs - Filter (C^+) (c) t=7 µs - Filter (C_2)

(d) t=8 µs - No filter (e) t=8 µs - Filter (C^+) (f) t=8 µs - Filter (C_2)

(g) t=9 µs - No filter (h) t=9 µs - Filter (C^+) (i) t=9 µs - Filter (C_2)

(j) t=10 µs - No filter (k) t=10 µs - Filter (C^+) (l) t=10 µs - Filter (C_2)

(m) t=11 µs - No filter (n) t=11 µs - Filter (C^+) (o) t=11 µs - Filter (C_2)

(p) t=12 µs - No filter (q) t=12 µs - Filter (C^+) (r) t=12 µs - Filter (C_2)

Figure 10. Pictures taken with high-speed camera and 2 different filters for U=1300 V, 4 capacitors, ctd.

IV.C. Derived values

With help of the discharge current and voltage waveforms, the energy transfer efficiency can be derived as the energy-normalized integral of the active power:[14]

$$\eta_{tran} = \frac{\int_0^\infty U(t) \cdot I(t)\, \mathrm{d}t}{E_0}. \tag{3}$$

For the thruster energies investigated, the calculated values are plotted in Figure 12.

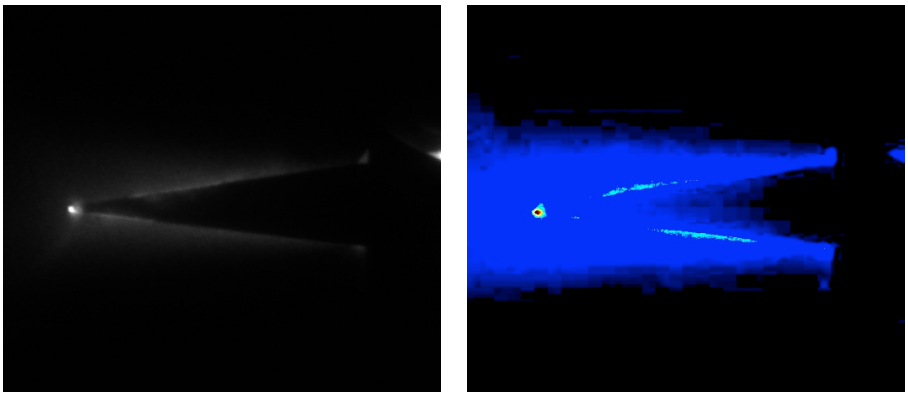

(a) Raw picture for first plasma phenomenon (b) Post-processed picture for first plasma phenomenon

Figure 11. View from downside on anode

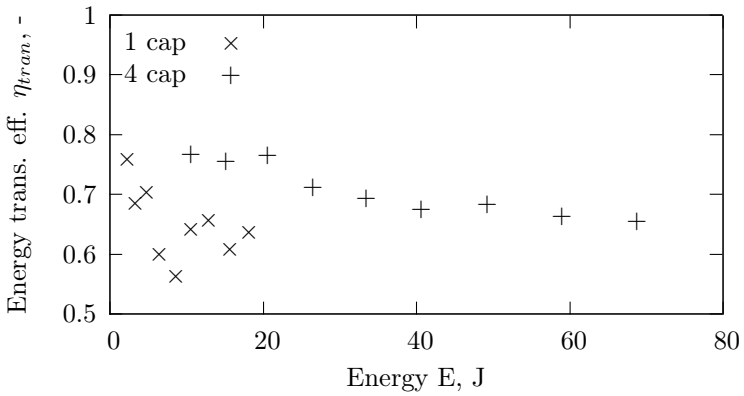

Figure 12. Energy transfer efficiencies for different thruster energies

The values between 56 and 77% compare well with values of 50 to 75% for the thruster of Palumbo and Guman[14] and the ≈70% for the thruster of Osaka Institute of Technology.[19] However, as for the acceleration efficiencies $\eta_{acc} = \eta_t/\eta_{tran}$, the values differ strongly for ADD SIMP-LEX, as can be seen in Figure 13. In general, it can be derived, that an increase in discharge voltage leads to a decrease in transfer efficiency whereas the acceleration efficiency might be positively influenced. However, not enough experimental data of the thrust efficiency were present to verify this theory.

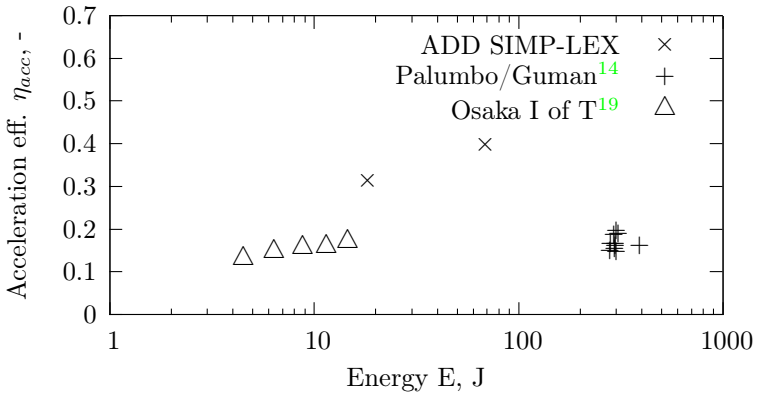

Figure 13. Acceleration efficiencies for different thrusters

Another efficiency to characterize PPT was introduced by Jahn,[20] named the electrical efficiency. The assumption herein is that the ohmic fraction of the used power is regarded as loss, and that the input power into the plasma only depends on the inductive part. Hence, it is defined as:

$$\eta_{el} = \frac{1}{2}\frac{\int_0^\tau I^2(t)\cdot \dot{L}(t)\,\mathrm{d}t}{E_0}. \tag{4}$$

Although, this efficiency might yield information about the transformation of electrical energy into kinetic energy of the plasma, it neglects dynamic losses and assumes a transfer efficiency of 100%. To compute this value for the thruster configurations investigated, it is necessary to combine the measured discharge current signal, the calculated change in inductance as a function of the position of the current sheet, and the measured plasma propagation velocity to transform the change in inductance into a function of time. As every of these values is affected by error sources, e.g., electromagnetic noise, calibration errors, measurement uncertainties, etc., these values have to be regarded cautiously. Table 3 shows some benchmark efficiencies computed for Add Simp-lex.

Table 3. Electrical efficiency for different thruster configurations, in %

	1 capacitor	4 capacitors
500 V	8.6	20.5
900 V	38.0	39.1
1300 V	22.6	23.7

The values do not change a lot for a change in capacitors, except for the low-energy case. Further, the maximum values are not found for the highest energies, but for the middle voltage. One possible explanation might be that the differences in plasma creation affect the energy exchange with the plasma. While an increase in voltage to 900 V ameliorates this exchange, the additional plasma creation during the 1300 V case reduces the efficiency again as more energy is going towards the ablation, dissociation and ionization of the propellant. To improve this discussion, a better definition of the efficiencies might be necessary, reducing the assumptions made. Further, a more reliable method to determine the plasma propagation speed might be necessary to improve the results shown.
Combining the information about the computed current-normalized magnetic flux density and the maximum discharge current yields a maximum value of about 4 T close to the electrodes, and 8 to 10 T close to the current sheet, for the highest-energy case. This is much higher compared to the 0.7 T measured for Simp-lex[10] implying a stronger acceleration of the plasma created and justifies the design changes made.

V. Conclusions and Outlook

Investigations of the discharge current and the plasma propagation for the pulsed plasma thruster Add Simp-lex were done successfully for different thruster configurations. A link between both results was seen in terms of number of plasma creations, brightness and creation of charged particles. Combination of both measurements towards an electrical efficiency was realized by means of the modeled change in inductance, enabling a possibility to compare the thruster configurations. The model was improved with regard to computation speed and convergence. Measurement of the propagation velocity for the plasma front was defied by several effects, and therefore, a more reliable measurement method would be desirable. To also enable verification of the computed magnetic flux densities, induction probe measurements are envisaged from which the plasma velocity can also be deducted.
The pictures taken with the high-speed camera indicate different distributions and compositions of the plasma species especially with regard to the ionization capability of later current extrema. Application of spectroscopic means to determine the composition and spatial distribution of these species would further improve the insight into the discharge processes.
The calculation of the energy transfer efficiencies indicate similar values if compared with previous other researches. Higher values were found for lower voltages, implying that the losses are more crucial at higher discharge energies. Regarding the electrical efficiency, higher values of about 40% were found at the middle voltage of 900 V. As seen from the high-speed camera pictures, almost only neutral particles are created during the negative current period, possibly reducing the efficiency of the energy conversion into the plasma.

For lower voltages, however, the current density in the discharge space might not be sufficient to "perfectly" create plasma, and, thus, suffering from losses due to a lower ionization degree. Again, spectroscopic measurements will help elucidate more accurately these observations.

Acknowledgments

T. Schönherr wants to thank the Japanese Ministry of Education, Culture, Sports, Science and Technology (*Monbukagakusho*) for the financial support of the PhD thesis, and M. Lau (IRS) for the discussion of the experimental setup and results.

References

[1]Bock, D., Herdrich, G., Lau, M., Schönherr, T., Wollenhaupt, B., and Röser, H.-P., "Electric Propulsion Systems for Small Satellites: The LEO Mission Perseus," *3rd European Conference for Aero-Space Sciences*, Versailles, France, July 2009.

[2]Herdrich, G., Bauder, U., Bock, D., Eichhorn, C., Haag, D., Lau, M., Schönherr, T., Stindl, T., Fertig, M., Löhle, S., Auweter-Kurtz, M., and Röser, H.-P., "Activities in Electric Propulsion Development at IRS," *Transactions JSASS Space Technology Japan*, Vol. 7, No. ists26, 2009, pp. Tb_5–Tb_14.

[3]Schönherr, T., Nawaz, A., Lau, M., Petkow, D., and Herdrich, G., "Review of Pulsed Plasma Thruster Development at IRS," *Transactions JSASS Space Technology Japan*, under review, 2010.

[4]Schönherr, T., Nawaz, A., Herdrich, G., Röser, H.-P., and Auweter-Kurtz, M., "Influence of Electrode Shape on Performance of Pulsed Magnetoplasmadynamic Thruster SIMP-LEX," *Journal of Propulsion and Power*, Vol. 25, No. 2, March-April 2009, pp. 380–386.

[5]Nawaz, A., Albertoni, R., and Auweter-Kurtz, M., "Thrust efficiency optimization of the pulsed plasma thruster SIMP-LEX," *Acta Astronautica*, Vol. 67, No. 3-4, August-September 2010, pp. 440–448.

[6]Schönherr, T., Komurasaki, K., Lau, M., Herdrich, G., Röser, H.-P., Yokota, S., and Arakawa, Y., "Cooperation Activities between IRS and the University of Tokyo in the Field of Pulsed Plasma Thruster Development," *31st International Electric Propulsion Conference*, Ann Arbor, MI, USA, September 2009.

[7]Nawaz, A., Bauder, U., Böhrk, H., Herdrich, G., and Auweter-Kurtz, M., "Electrostatic Probe and Camera Measurements for Modeling the iMPD SIMP-LEX," *43rd AIAA/ASME/SAE/ASEE Joint Propulsion Conference and Exhibit*, Cincinnati, OH, USA, July 2007.

[8]Nawaz, A., *Entwicklung und Charakterisierung eines gepulsten instationären MPD Triebwerks als Primärantrieb für Weltraumsonden*, Dissertation, Universität Stuttgart, Stuttgart, Germany, February 2010.

[9]Schönherr, T., Komurasaki, K., Kawashima, R., Arakawa, Y., and Herdrich, G., "Effect of Capacitance on Discharge Behavior of Pulsed Plasma Thruster," *Journal of IAPS*, Vol. 18, No. 1, (under review) 2010.

[10]Nawaz, A., Lau, M., Herdrich, G., and Auweter-Kurtz, M., "Investigation of the Magnetic Field in a Pulsed Plasma Thruster," *AIAA Journal*, Vol. 46, No. 11, November 2008, pp. 2881–2889.

[11]Clenshaw, C. W. and Curtis, A. R., "A method for numerical integration on an automatic computer," *Numerische Mathematik*, Vol. 2, No. 1, December 1960, pp. 197–205.

[12]Popov, G. A. and Antropov, N. N., "Ablative PPT. New Quality, New Perspectives," *Acta Astronautica*, Vol. 59, No. 1-5, July-September 2006, pp. 175–180.

[13]Burton, R. L. and Turchi, P. J., "Pulsed Plasma Thruster," *Journal of Propulsion and Power*, Vol. 14, No. 5, September-October 1998, pp. 716–735.

[14]Palumbo, D. J. and Guman, W. J., "Propellant Sidefeed-Short Pulse Discharge Thruster Studies," Technical Report NASA CR-112035, Fairchild Industries Inc., Farmingdale, NY, USA, January 1972.

[15]Thomas, R. E., Burton, R. L., and Polzin, K. A., "Gallium Electromagnetic (GEM) Thruster Performance Measurements," *31st International Electric Propulsion Conference*, Ann Arbor, MI, USA, September 2009.

[16]Palumbo, D. J. and Guman, W. J., "Effects of Propellant and Electrode Geometry on Pulsed Ablative Plasma Thruster Performance," *Journal of Spacecraft and Rockets*, Vol. 13, No. 3, March 1976, pp. 163–167.

[17]Guman, W. J., "Pulsed plasma technology in microthrusters," Technical Report AFAPL-TR-68-132, Fairchild Hiller Corp./Republic Aviation Division, Wright-Patterson AFB, OH, USA, November 1968.

[18]Palumbo, D. J. and Guman, W. J., "Pulsed Plasma Propulsion Technology," Technical Report AD-768224, Fairchild Industries Inc., Farmingdale, NY, USA, September 1973.

[19]Edamitsu, T. and Tahara, H., "Study on Performance Enhancement of an Electrothermal Pulsed Plasma Thruster," *Journal of High Temperature Society (in Japanese)*, Vol. 31, No. 5, 2005, pp. 291–298.

[20]Jahn, R. G., *Physics of Electric Propulsion*, Dover Publications, Inc., Mineola, NY, USA, 2006.